Complex Transport Phenomena in a Simple Lattice Gas System

Akinori Awazu[*]

Department of Physics, University of Tokyo,

Hongou 7-3-1, Bunkyou-ku, Tokyo 113-0033, Japan.

(Dated: February 6, 2008)

Abstract

The transport phenomena of a nonequilibrium lattice gas system are investigated. We consider a simple system that consists of two particles interacting repulsively and the potential forces acting on these particles. Under an external driving field applied to only one particle, we found the following relation between the mean velocity of the driven particle and the coefficient of effective drag of this particle under certain conditions; With the increase in the mean velocity, the coefficient of effective drag varies in the form, increase → decrease → increase → decrease. Moreover, under other conditions, we found the following relations between these values which show changes similar to those between shear rate and shear viscosity observed in the shear-thickening polymer or colloidal suspensions; With the increase in the mean velocity, the coefficient of effective drag varies in the form, increase → decrease or decrease → increase → decrease. We explain the mechanisms of such phenomena by considering the transition diagrams.

PACS numbers: 05.60.-k, 83.10.-y, 47.50.+d

---

[*] E-mail address: awa@daisy.phys.s.u-tokyo.ac.jp

INTRODUCTION

Nonequilibrium lattice gases are simple mathematical models, which have been useful and important in studies of the several properties of nonequilibrium systems with numerous degrees of freedom[1]. Recently, many varieties of nonequilibrium phenomena such as nonequilibrium phase transitions[2], a variety of particle flows[3, 4, 5, 6], appearances of long-range spatial correlations[7, 8], and the mathematical foundations of nonequilibrium statistical mechanics and thermodynamics[9, 10, 11, 12] have been investigated through such lattice gases.

In this paper, we investigate the transport behaviors of a lattice gas system with a periodic boundary, which consists of only two particles interacting repulsively and the potential forces acting on them. Under nonequilibrium conditions, lattice gas systems have been known to show some nontrivial phenomena, such as the appearance of long-range spatial correlations[8] and anomalous drift motions[6], even if the system involves only two particles.

In our system, the following complex transport properties are found when only one particle is driven by an external driving field; With the increase in the mean velocity of the driven particle, the coefficient of effective drag of this particle (=[driving field strength]/[mean velocity]) varies in the form, increase → decrease → increase → decrease under certain conditions. Moreover, under other conditions, the relation between these values show changes similar to those between shear rate and shear viscosity observed experimentally in the shear-thickening polymer[14, 15, 16] or colloidal suspensions[21, 22]; With the increase in the mean velocity, the coefficient of effective drag varies in the form, increase → decrease or decrease → increase → decrease.

In the following sections, details of the numerical and analytical results are shown. First, we introduce our model and show the numerical results, where the above-mentioned phenomena are observed. Next, we explain the mechanism of these phenomena by considering the transition diagrams. Last, we show the similarities between our obtained results and those observed in the polymer solutions or colloidal suspensions.

MODEL

Now, we introduce a lattice gas model, which is the same as that studied in our previous paper[6]. We consider a lattice system with two parallel one-dimensional lanes where each lane involves L sites with a periodic boundary. Each lane contains only one particle which moves randomly to the nearest sites without changing lanes. The sites occupied by particles in the 1st and 2nd lanes are denoted x_1 and x_2, respectively, which are given as integer numbers from 0 to $L-1$.

The effect of potential forces acting on the particles is described by the following Hamiltonian:

$$H(x_1, x_2) = V(x_1) + V(x_2) + V_{12}(x_1, x_2), \tag{1}$$

where $V(x)$ represents the one-body potential on each lane, and $V_{12}(x_1, x_2)$ represents the interaction potential between the two particles. Furthermore, an external driving field is applied to the particle on the 2nd lane. We denote the field strength F.

The time evolution of this system is described by the iteration of the following three steps. First, one of the two particles is randomly chosen. Let the position of the chosen particle be x. Second, its neighboring site y, $x-1$ or $x+1$, is randomly chosen. Third, the chosen particle moves from x to y with the following probability

$$c(x, y; x_1, x_2) = \frac{1}{1 + \exp[Q(x \to y; x_1, x_2)/k_B T]}, \tag{2}$$

with

$$Q(x \to y; x_1, x_2) = H(x_1', x_2') - H(x_1, x_2) - F(x_2' - x_2), \tag{3}$$

where $(x_1', x_2') = (x_1, y)$ when $x = x_2$, and $(x_1', x_2') = (y, x_2)$ when $x = x_1$[13]. T is temperature and the Boltzmann constant k_B is set 1. Here, the time step is given by [No. of above iterations]/[No. of particles (= 2)].

Specifically, we study the case where $V(x) = V|L/2 - x|$ (Fig. 1), and $V_{12}(x_1, x_2) = I\delta_{x_1, x_2}$ using the $L \times L$ unit matrix δ_{ij}. Also, we focus on the case $L = 4$. We found that this size is the minimum required to exhibit the phenomenon we demonstrate in the presented paper.

SIMULATION RESULTS

In this section, we show the simulation results of this system. We mainly focus on the cases with $V < I$ and $|F| < I+V$ because we obtained some novel phenomena as shown in the belows. Such conditions indicate that the influences of the potential forces and the driving field are weak compared to those of the particle-particle interactions. In order to characterize the system, we define the mean velocity of the driven particle (in the 2nd lane) in steady state, u, as the difference of the long time average of the moving ratio of the driven particle in the positive and negative directions. Here, the direction $x_i : 0 \to 1 \to ... \to (L-1) \to 0 \to$ is positive. For simplicity, $I = 1$ and $F > 0$ are set.

First, we focus on the cases where T is small enough compared to I. Figures 2(a), (b) and (c) show u as a function of F for (a) $V = 0.25$ with $T = 0.05$ or $T = 0.07$, (b) $V = 0.4$ with $T = 0.05$ or $T = 0.08$, and (c) $V = 0.6$ with $T = 0.08$ or $T = 0.1$. Then, the following two types of $F - u$ profiles appear; A) u increases slowly $\to$ steeply $\to$ slowly $\to$ steeply with the increase in F as shown in (a) and (b) with a smaller T. B) u increases steeply $\to$ slowly $\to$ steeply with the increase in F as shown in (b) with a larger T and (c).

From these results, the relations between u and the coefficient of effective drag of the driven particle, η, defined as F/u are straightforwardly obtained. Figures 3(a), (b) and (c) show η as a function of u for (a) $V = 0.25$ or $V = 0.3$, (b) $V = 0.35$ or $V = 0.4$, and (c) $V = 0.55$ or $V = 0.6$. Here, the properties of $u - \eta$ profile change depending on V and T as following.

I) -i) In the case with $V < I/3$, as shown in Fig. 3(a), η varies in the form, increase $\to$ decrease $\to$ increase $\to$ decrease, with the increase in u for small T (for example $T = 0.05$). -ii) On the other hand for a little larger T (for example $T = 0.07$), the change in η becomes less sharp and changes in the form, increase $\to$ fast decrease $\to$ slow decrease $\to$ fast decrease, with the increase in u. Here, u at the maximum values of η decrease with the increase in V or the decrease in T.

II) -i) In the case with $I/3 < V < I/2$, as shown in Fig. 3(b), η varies in the form, increase $\to$ decrease $\to$ increase $\to$ decrease, with the increase in u for small T (for example $T = 0.05$). -ii) On the other hand for a little larger T (for example $T = 0.08$), the change in η becomes less sharp, and simpler in the form, decrease $\to$ increase $\to$ decrease, with the increase in u. Here, u at the maximum values of η decrease with the increase in V or the

decrease in T.

III) In the case with $I/2 < V$, as shown in Fig. 3(c), η varies in the form, decrease $\rightarrow$ increase $\rightarrow$ decrease, with the increase in u independently of T. Here, u at the maximum values of η decrease with the decrease in V or T.

It is remarkable that the $u - \eta$ profile given in case I-ii) appears qualitatively similar to that between the shear rate and shear viscosity coefficient of the shear-thickening polymer solutions obtained experimentally[14, 15, 16]. On the other hand, in the case II-ii) or III), the $u - \eta$ profile appear qualitatively similar to that between the shear rate and shear viscosity coefficient of the shear-thickening colloidal suspension obtained experimentally[21, 22].

Phase diagram for the properties of $u - \eta$ profile as functions of V and T is given as Fig. 3(d). Here, the boundaries given as $V = I/3$ and $V < I/2$ (as indicated by the broken lines.) are predicted by the analytical studies as mentioned in the next section. If T is given larger, $u - \eta$ profiles for several V become less sharp and close to flat like Newtonian fluid continuously as shown in Fig. 3(a), (b) and (c) (for example $T = 0.2$ or $T = 0.32$).

It is noted that, if $V >> I$ in which the particle-particle interactions are much smaller than any other effects, u is roughly estimated as $\propto \exp(-(2V - I - F)/T) - \exp(-(2V - I + F)/T)$. In such cases, η decreases monotonically with the increase in u for small T, and $\eta - u$ profile closes to flat with the increase in T. Thus, the particle-particle interactions play important roles to show the presented non-trivial behaviors like those observed shear-thickening solutions.

ANALYSIS OF THE MODEL BY TRANSITION DIAGRAMS

In this section, we try to explain the mechanism of our obtained phenomena by considering the transition diagrams.. First, we name all states of this system using the sites occupied by the particles in each lane (x_1, x_2). Since $L = 4$, this system has 16 states from $(0, 0)$ to $(3, 3)$. The transitional tendency from (x_1, x_2) to (x'_1, x'_2) is given by $Q(x \rightarrow y; x_1, x_2)$, which was defined previously. Here, $(x'_1, x'_2) = (x_1, y)$ when $x = x_2$, and $(x'_1, x'_2) = (y, x_2)$ when $x = x_1$. Then, we obtain the transition diagrams; including all information on the transitions between states.

We focus on the F dependent changes of the transition diagrams. Figure 4 shows the typical transition diagrams in the cases where (a) $F < V$, (b) $V < F < I - 2V$, (c)

$I - 2V < F < I - V$, (d) $I - V < F < I$ and (e) $I < F$ under $V < I/3$. Here, (i, j) indicates the state (x_1, x_2), the arrows give the direction of the transition with a probability higher than ~ 0.5 implying $Q(x \to y; x_1, x_2) \stackrel{<}{\sim} 0$, and the values beside these arrows indicate the value of $|Q(x \to y; x_1, x_2)|$. The motion of the system is represented by the random walk caused by the fluctuation with T in the transition diagram. Here, the transition in a vertical direction indicates the motion of the particle in the 1st lane, and that in a horizontal direction indicates the motion of the driven particle in the 2nd lane.

As shown in Figs. 4, there exist two types of states, the transient state, which has some arrows directing to some other states, and the attractor, which has no arrows directing to any other states. If T is small enough compared to I and V, the transitions from each state are considered to conform to the following tendencies in most cases. 1) From the transient states, one of all transitions with the arrows directing to any other of the states is realized randomly. 2) From the attractors, only a transition in the direction with the smallest $|Q(x \to y; x_1, x_2)|$ $(= |Q_{min}|)$ is realized with the probability $\sim \exp(-Q_{min}/T)$ (escape rate). It is noted that the system tends to stay the attractors for most of the time. Thus, the escape rate from these attractors contributes dominantly to give the mean velocity of the driven particle u.

Now, we focus on the typical trajectories in the transition diagrams for the cases with $V < I/3$ (Figs. 4) to explain the appearance of the $F - u$ relations like in Fig. 2(a). When $F < V$, the transition diagram as given in Fig. 4(a) involves the following trajectory as a typical one characterizing the steady state motion, $(1, 2) \to (1, 3) \to (2, 3) \to (2, 0) \to (2, 1) \to (3, 1) \to (3, 2) \to (0, 2) \to (1, 2)$. (as indicated by thin arrows). This trajectory indicates the motions in which both particles proceed in the direction of F. Here, this involves four attractors, $(1, 2)$, $(2, 3)$, $(2, 1)$ and $(3, 2)$. The escape rates from the attractors $(1, 2)$ or $(2, 3)$ given through the transitions $(1, 2) \to (1, 3)$ or $(2, 3) \to (2, 0)$ increase with the increase in F. However, those of $(2, 1)$ or $(3, 2)$ given through the transitions $(2, 1) \to (3, 1)$ or $(3, 2) \to (0, 2)$ are independent of F. Then, u cannot increase so fast with F in this case.

In the case where $V < F < I - 2V$, the typical trajectories giving the steady state motions still involve the attractors $(2, 1)$ and $(3, 2)$ as shown in Fig. 4(b) (as indicated by thin arrows). Also in this case, the escape rates from these attractors are still independent of F. In this case, u increases little with F.

In the case where $I - 2V < F < I - V$, the following two types of typical trajectories

6

appear, as shown in Fig. 4(c), i) trajectories including two attractors, $(2, 1)$ and $(3, 2)$, for example $(1, 2) \rightarrow (1, 3) \rightarrow (2, 3) \rightarrow (2, 0) \rightarrow (2, 1) \rightarrow (2, 2) \rightarrow (3, 2) \rightarrow (0, 2) \rightarrow (1, 2)$ (as indicated by thin arrows), and ii) trajectories including only one attractor $(2, 1)$ for example $(2, 1) \rightarrow (2, 2) \rightarrow (2, 3) \rightarrow (2, 0) \rightarrow (2, 1)$ (as indicated by broken arrows). Here, the former trajectory indicates the motions in which both particles proceed in the direction of F while the latter indicates the motions in which only the driven particle proceeds. In this case, the escape rate from $(2, 1)$ given through the transition $(2, 1) \rightarrow (2, 2)$ increases exponentially with the increase in F while the escape rate $(3, 2)$ given through the transition $(3, 2) \rightarrow (0, 2)$ is independent of F. Then, the mean velocity of the driven particle remains unaffected by the increase in F if the system develops along trajectories i). On the other hand, this increases exponentially with F if the system develops along trajectories ii). Thus, within this range of F, u increases steeply with F on the average.

In the case where $I - V < F < I$, similar to the previous case, the following two types of trajectories are still typical ones as shown in Fig. 4(d), i) trajectories including two states, $(2, 1)$ and $(3, 2)$ (as indicated by thin arrows), and ii) trajectories including a state $(2, 1)$, but not including a state $(3, 2)$ (as indicated by broken arrows). However, the state $(2, 1)$ is no longer the attractor although $(3, 2)$ is still an attractor. Then, the diagram includes trajectories involving an attractor $(3, 2)$ and those involving no attractors. In the former trajectories, the escape rate from $(3, 2)$ is still independent of F. Therefore, u increases slightly with F.

In the case where $I < F(< I + V)$, the escape rate from the attractor $(3, 2)$ becomes one increasing exponentially with F, which is given through the transition $(3, 2) \rightarrow (3, 3)$ as in Fig. 4(e). Then, the mean velocity of the driven particle along trajectories including the attractor $(3, 2)$ (as indicated by thin arrows) increases exponentially with F, although that along any trajectories without the attractor $(3, 2)$ (as indicated by broken arrows) are unaffected by F. Therefore, within this range of F, u increases steeply with F.

Thus, for $V < I/3$, u increases slowly $\rightarrow$ steeply $\rightarrow$ slowly $\rightarrow$ steeply with the increase in F. This result is consistent to the $F - u$ relations in Fig. 2(a).

In cases with $I/3 < V < I/2$ or $I/2 < V$, the manner of the F dependent changes of the transition diagrams proceed differently from the previous case. (We do not show the diagrams for such V in order to avoid the complications.) We can also explain the mechanism of the phenomena observed in each range of V via the same analytic method.

SUMMARY AND DISCUSSIONS

In this paper, we investigated the transport phenomena of a simple nonequilibrium lattice gas system. We measure the mean velocity of the driven particle (u) and the coefficient of effective drag of this particle (η). Under the certain ranges of parameters, we obtained the u - η relations qualitatively similar to the relations which observed between the shear rate and shear viscosity coefficient in the shear-thickening polymer solutions[14, 15, 16] or that of the shear-thickening colloidal suspensions[21, 22]. The mechanisms of these phenomena are explained by the transition diagram.

Now, we consider the similarities between our results and those obtained recent studies for the rheology of soft matter systems in a little more detail. The soft glassy systems like polymer solutions or colloidal suspensions under shear have been studied extensively by experiments, molecular dynamics simulations, the analysis of the transient network model or the random spin model, and studies of the mode coupling theory or an analysis of the pair distribution function[14, 15, 16, 17, 18, 19, 20, 21, 22, 23, 24, 25, 26].

Among results of some experimental and theoretical studies for shear-thickening polymer solutions, it has been observed that the shear viscosity varies in the form, increase $\rightarrow$ fast decrease $\rightarrow$ slow decrease $\rightarrow$ fast decrease, with the increase in the shear rate[14, 18]. Such a profile was obtained in the $u - \eta$ relation in our simulation under a certain condition (for the case I-ii in the phase diagram Fig. 3(d)). On the other hand, among results of some experimental and theoretical studies for shear-thickening colloidal suspensions, it has been observed that the shear viscosity varies in the form, decrease $\rightarrow$ increase $\rightarrow$ decrease, with the increase in the shear rate[21, 22, 23, 24, 25, 26]. Such a profile was also obtained in the $u - \eta$ relation in our simulation under the other certain conditions (for the case II-ii or III in the phase diagram Fig. 3(d)).

Moreover, among results of recent studies, the power law [shear viscosity coefficient] $\sim$ [shear rate]$^{-\delta}$ has been observed in the shear-thinning regime. Here, $\delta \sim 2/3$ has been given in some experimental studies, simulations and theoretical studies[22, 23, 24, 26] while δ that varies depending on several conditions between 0 and 1 has been obtained in the other experimental and theoretical studies[17, 21, 25]. On the other hand, we obtained the following $u - \eta$ relations in the η decreasing regime for lower T; $\eta \sim u^{0 \sim -0.5}$ for smaller u and $\eta \sim u^{-0.9}$ for larger u.

Thus, we expect our results to provide important hints to uncover the possible mechanism for several rheological characteristics of several soft materials. However, the relations of some properties, for example the exponents of the transport coefficients, the transport properties in cases with lower temperature, etc. are still unclear between our results and those obtained in several recent studies. Then, studies of extended models, including more lanes or particles in the space with more sites or continuous space, and the comparisons between such toy systems and either real systems or more realistic models of the polymer or colloidal systems represent important future issues.

---

[1] B. Schimttmann and R. K. P. Zia, Statistical Mechanics of Driven Diffusive Systems (Academic Press, London, 1995).

[2] S. Katz, L. J. Lebowitz and H. Spohn, J. Stat. Phys. **34** (1984) 497.

[3] B. Derrida, Phys. Rep. **301** (1998) 65.

[4] S. Takesue, T. Mitsudo and H. Hayakawa; Phys. Rev. E **68** (2003) 015103.

[5] V. Popkov and G M. Sch$\ddot{u}$tz, J. Stat. Phys. **112** (2003) 523.

[6] A. Awazu, J. Phys. Soc. Jpn. **74** (2005) 3127.

[7] P. Garrido, L. J. Lebowitz, C. Maes and H. Spohn, Phys. Rev. A **42** (1990) 1954.

[8] H. Tasaki, cond-mat/0407262

[9] J. Lebowitz and H. Spohn, J. Stat. Phys. **95** (1999) 333.

[10] H. Spohn, Large Scale Dynamics of Interacting Particles (Springer-Verlag, Berlin, 1991).

[11] B. Derrida, J. Lebowitz and E. R. Speer, Phys. Rev. Lett. **89** (2002) 030610.

[12] K. Hayashi and S. Sasa, Phys. Rev. E **68** (2003) 035104.

[13] $Q(x \to y; x_1, x_2) = H(x_1, 0) - H(x_1, x_2) - F$ holds when $x = x_2 = L - 1$ and $y = x + 1$, and $Q(x \to y; x_1, x_2) = H(x_1, L - 1) - H(x_1, x_2) + F$ holds when $x = x_2 = 0$ and $y = x - 1$.

[14] K. C. Tam, R. D. Jenkins, M. A. Winnik and D. R. Bassett, Macromolecules **31** (1998) 4149.

[15] S X. Ma and S L. Cooper, Macromolecules **34** (2001) 3294.

[16] J.-F. Berret, Y. Serero, Phys. Rev. Lett. **87** (2001) 048303.

[17] G. Marrucci, S. Bhargava and S L. Cooper, Macromolecules **26** (1993) 6483.

[18] A. Vaccaro and G. Marrucci, J. Non-Newtonian Fluid Mech. **92** (2000) 261.

[19] T. Indei, T. Koga and F. Tanaka, Macromol Rapid. Commun. **26** (2005) 701.

[20] T. Koga and F. Tanaka Euro. Phys. J. **E17** (2005) 115

[21] R. L. Hoffman, J. Colloid. Interfase Sci. **46** (1974) 491.

[22] E. Bertrand, J. Bibette and V. Schmitt, Phys. Rev. E **66** (2003) 060401.

[23] L. Berthier and J.-L. Barrat, J. Chem. Phys. **116** (2002) 6228.

[24] M. Sellitto and J. Kurchan, cond-mat/0507128.

[25] M. Fuchs and M. E. Cates, Phys. Rev. Lett. **89** (2002) 248304.
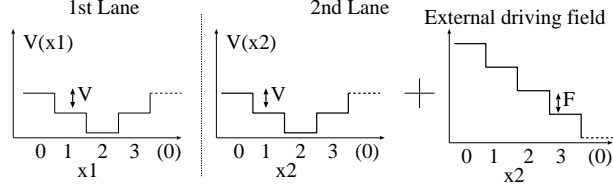
[26] M. Otsuki and S. Sasa, cond-mat/0511111.

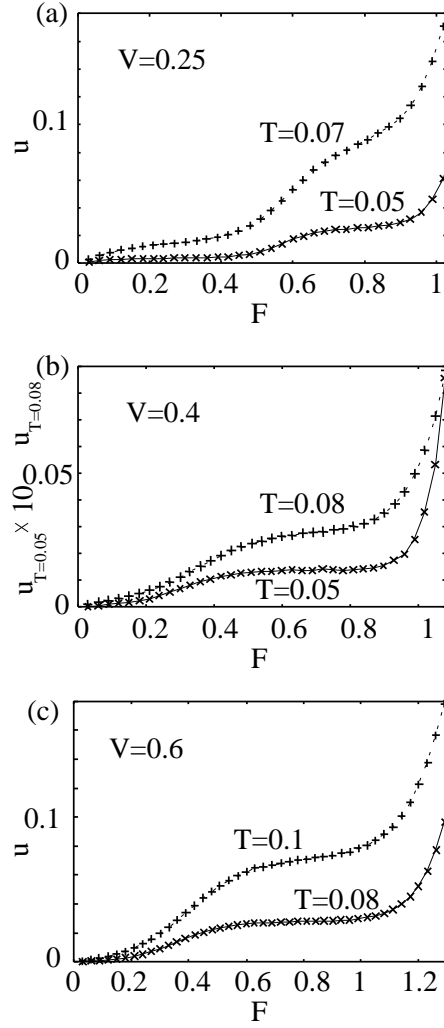FIG. 1: Illustrations of effects of potential and external field in each lane.

FIG. 2: Mean velocity u as a function of F for (a) $V = 0.25$ with $T = 0.05$ or $T = 0.07$, (b) $V = 0.4$ with $T = 0.05$ or $T = 0.08$ and (c) $V = 0.6$ with $T = 0.08$ or $T = 0.1$.
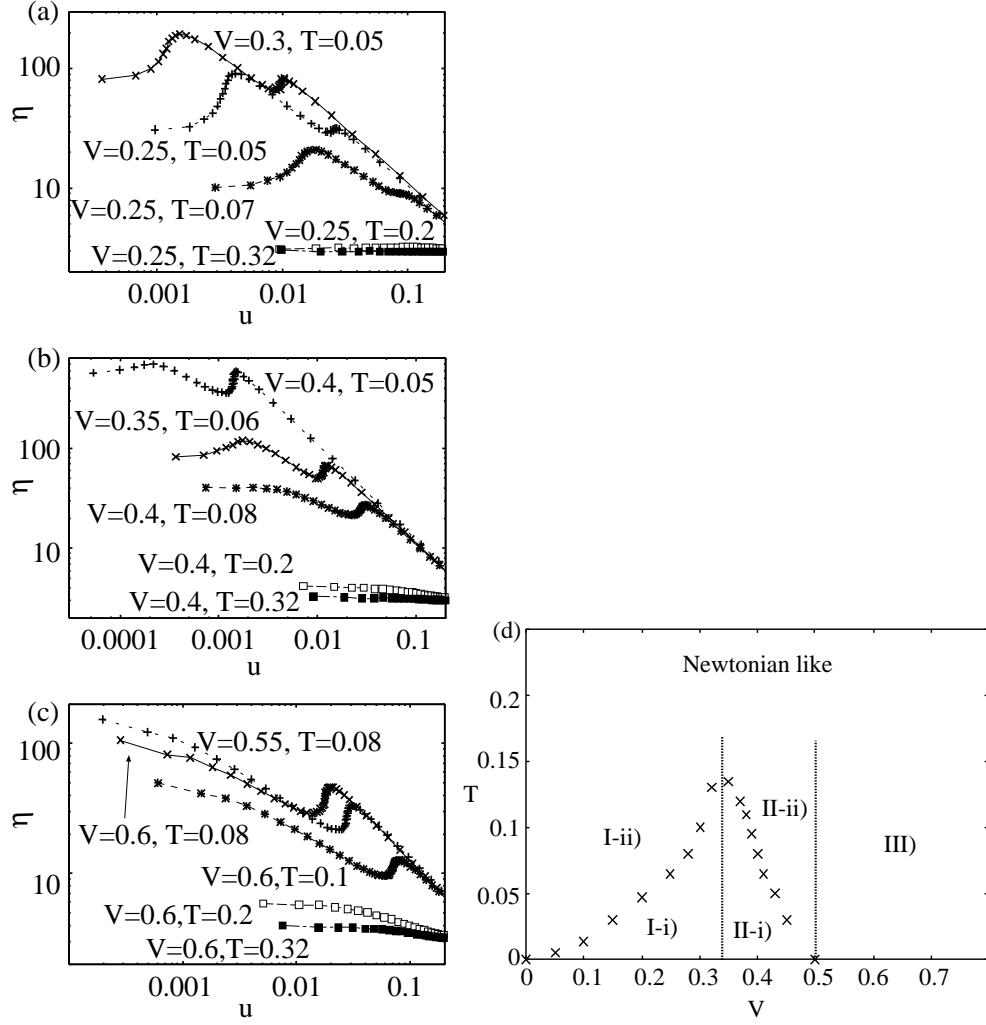
FIG. 3: Coefficient of effective drag η as a function of u for (a) $V = 0.3$ with $T = 0.05$ (Times) and $V = 0.25$ with $T = 0.05$ (Plus), $T = 0.07$ (Star), $T = 0.2$ (Empty square) or $T = 0.32$ (Full Square), (b) $V = 0.35$ with $T = 0.06$ (Times) and $V = 0.4$ with $T = 0.05$ (Plus), $T = 0.08$ (Star), $T = 0.2$ (Empty square) or $T = 0.32$ (Full Square) and (c) $V = 0.55$ with $T = 0.08$ and $V = 0.6$ (Times) with $T = 0.08$ (Plus), $T = 0.1$ (Star), $T = 0.2$ (Empty square) or $T = 0.32$ (Full Square). (d) Phase diagram of the system as functions of V and T. Dots and broken lines give the boundaries between states
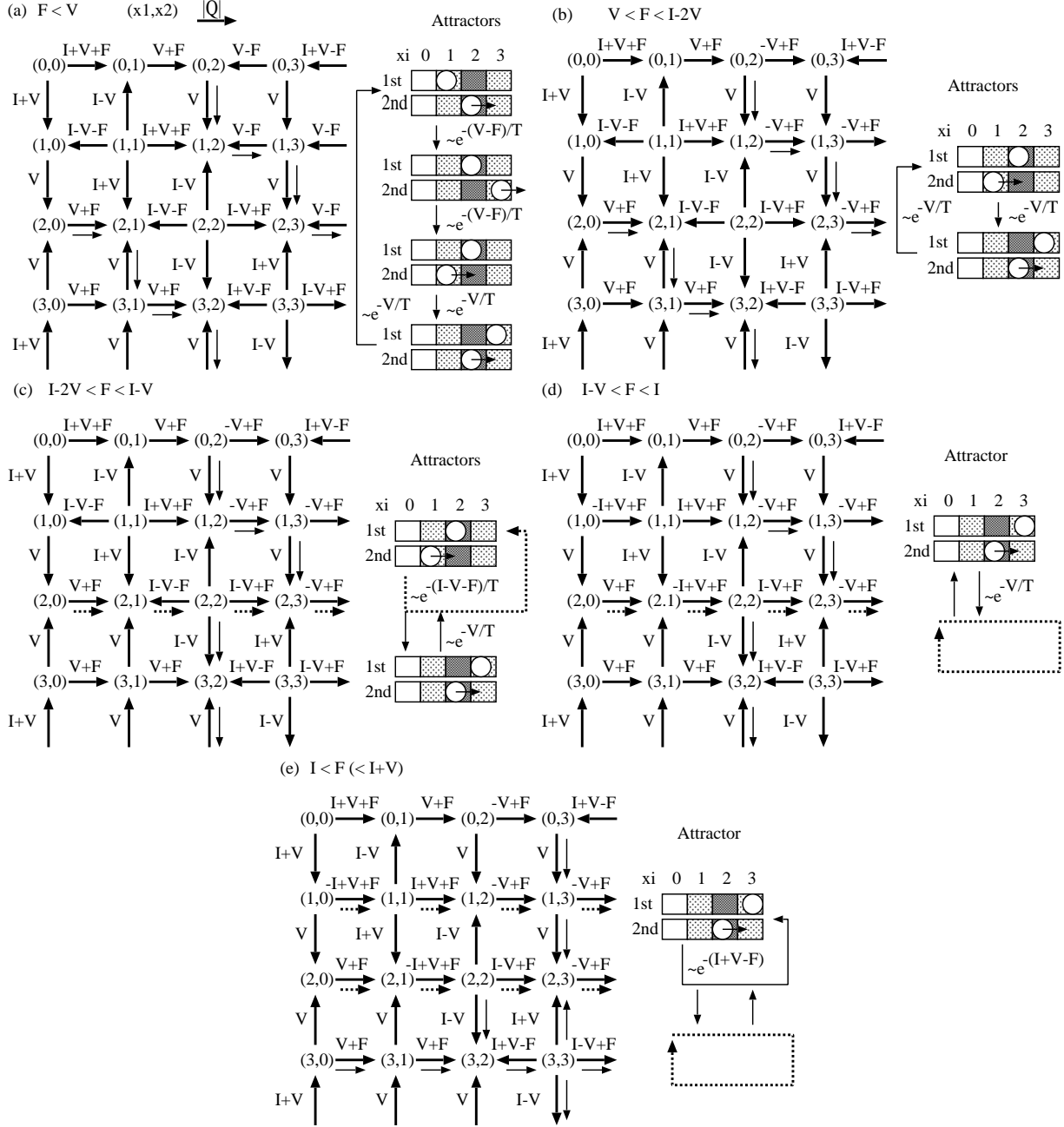
FIG. 4: Typical transition diagram (left), and illustrations of attractors and rough estimated escape rates from them (right) for (a)$F < V$, (b)$V < F < I - 2V$, (c)$I - 2V < F < I - V$, (d)$I - V < F < I$ and (e)$I < F < I + V$ under $V < I/3$.